Geodesic calculation of color difference formulas and comparison with the Munsell color order system

Dibakar Raj Pant[1,2] and Ivar Farup[1]

[1]The Norwegian Color Research Laboratory,
Gjøvik University College, Norway
[2]The Laboratoire Hubert Curien,
University Jean Monnet, Saint Etienne, France

Abstract

Riemannian metric tensors of color difference formulas are derived from the line elements in a color space. The shortest curve between two points in a color space can be calculated from the metric tensors. This shortest curve is called a geodesic. In this paper, the authors present computed geodesic curves and corresponding contours of the CIELAB (ΔE_{ab}^*), the CIELUV (ΔE_{uv}^*), the OSA-UCS (ΔE_E) and an infinitesimal approximation of the CIEDE2000 (ΔE_{00}) color difference metrics in the CIELAB color space. At a fixed value of lightness L^*, geodesic curves originating from the achromatic point and their corresponding contours of the above four formulas in the CIELAB color space can be described as hue geodesics and chroma contours. The Munsell chromas and hue circles at the Munsell values 3, 5 and 7 are compared with computed hue geodesics and chroma contours of these formulas at three different fixed lightness values. It is found that the Munsell chromas and hue circles do not the match the computed hue geodesics and chroma contours of above mentioned formulas at different Munsell values. The results also show that the distribution of color stimuli predicted by the infinitesimal approximation of CIEDE2000 (ΔE_{00}) and the OSA-UCS (ΔE_E) in the CIELAB color space are in general not better than the conventional CIELAB (ΔE_{ab}^*) and CIELUV (ΔE_{uv}^*) formulas.

Introduction

In a color space, color differences are described as the distance between two color points. This distance gives us a quantitative value which in general should agree with perceptual color differences. We can describe such distances from different geometrical points of view. For example, the CIELAB color space is isometric to the Euclidean geometry and the distance is described by the length of a straight line because it has zero curvature everywhere. The distance is no longer the length of a straight line, if we model a color space as a Riemannian space having nonzero curvature. In such a space, the curve having the shortest length or distance between any two points is called a geodesic. The aim of

a color space and a color difference formula is to give a quantitative measure (ΔE) of the perceived color difference correctly. The development of many color spaces and color difference formulas are outcomes of a number of studies of visual color differences based upon the distribution of color matches about a color center [1–5]. Many research works in the past have been continuing to relate theoretical models of color differences with experimental results.

Helmholtz [6] was the first to derive a line element for a color space as a Riemannian space. Schrödinger [7] modified Helmholtz's line element stating that the additivity of brightness is essential for the formulation of the line element. He further argued that surfaces of constant brightness can be derived from the line element in the following way: Suppose that p_1 and p_2 represent the coordinates of two color stimuli in a tristimulus space, p_1 moves away from the origin along a straight line in that space, and p_2 remains fixed. When the geodesic distance between p_1 and p_2 is at minimum, the two given color stimuli are said to be equally bright (which in modern parlance means they are equally luminous). The geodesic between the final p_1 and p_2 is called a constant-brightness geodesic.

Muth et al. [8] used Schrödinger's theoretical conjecture to compute constant brightness color surfaces in the xyY space for FMC1 and FMC2 color difference formulas. The shape of this computed constant brightness surface is consistent with experimental results. Jain [9] determined color distance between two arbitrary colors in the xyY space by computing the geodesics. He also found that geodesics and the constant brightness contours are in agreement with the experimental results of Sanders and Wyszecki [10]. A thorough review of color metrics described with the line element can be found in [11–14].

Wyszecki and Stiles [14] hypothesized that all colors along a geodesic curve originating from a point representing an achromatic stimulus on a surface of constant brightness share the same hue. They further hypothesized that contours of constant chroma can be determined from these geodesics (henceforth called hue geodesics) by taking each point on a chroma contour as the terminus of a hue geodesic such that all the hue geodesics terminate on that chroma contour at the same geodesic distance. This construct has also been used to compute the curvature of color spaces by Lenz at el. [15]. Many other researchers have also pointed out that hue geodesics play a vital role in various color-imaging applications such as color difference preserving maps for uniform color spaces, color-weak correction and color reproduction [15–18].

Hue geodesics and chroma contours of color difference formulas are useful to study the perceptual attributes hue, chroma and lightness predicted by the color difference metric theoretically. A color order system like the Munsell is described in terms of hue, chroma and value to represent scales of constant hue, chroma and lightness. This is analogous to the Riemannian coordinate system. This analogy provides us to compare hue geodesics and chroma contours of a color difference formula in a color space with respect to the Munsell chromas and hues circles computed at a fixed value of lightness which should correspond to the Munsell value. In this sense, in the CIELAB color space, hue geodesics starting from the origin of a^*, b^* at a fixed value of lightness L^* are corresponding to the curves of increasing or decreasing Munsell chroma starting from the same origin at constant hue. In a similar way, chroma contours are closed curves with a constant hue geodesic distance from the achromatic origin. They are also corresponding to changing Munsell hue circles from the origin at the constant

chroma.

The CIELAB and the CIELUV [19] color difference formulas are defined by Euclidean metrics in their own color spaces. The CIEDE2000 [20] is an improved non-Euclidean formula based on the CIELAB color space. The ΔE_E proposed by Oleari [21] is a recent Euclidean color difference formula based on the OSA-UCS color space. However, all these color spaces do not have sufficient perceptual uniformity to fit visual color difference data [22–28]. This leads to difficulty in determining the maximum performance of color difference formulas for measuring visual color differences. Computing hue geodesics and chroma contours of these formulas in a color space help to evaluate their perceptual uniformity theoretically. Similarly, hue geodesics have to be calculated to study distribution of the color stimuli of a color difference formula in a color space. To calculate large color differences, hue geodesics have to calculated [14, 29]. This is even crucial for formulas like the CIEDE2000 because they are developed to measure small color differences, 0–5 ΔE_{ab}^* [20].

In this paper, the authors test the hypothesis described in the fourth paragraph by computing the hue geodesics and chroma contours of four color difference formulas, the CIELAB, the CIELUV, the Riemannian approximation of CIEDE2000 [30] and the OSA-UCS based ΔE_E in the CIELAB color space, and comparing the results to the Munsell color order system. The mathematical construct to compute these hue geodesics and chroma contours using Riemannian metric tensors of each formula are given in the section "The geodesic equation". They are computed at a fixed value of lightness L^*, starting from the origin of the a^*, b^* plane. For the first three color difference metrics above, constant L^* correspond to the constant brightness surface according to Schrödinger's criterion. For the OSA-UCS based ΔE_E it does not correspond to constant brightness due to the definition of the OSA-UCS space. Different hue geodesics and chroma contours of the above four formulas are computed taking three different fixed values of lightness, L^*, corresponding to the Munsell values 3, 5 and 7. The Munsell chromas and hue circles are also plotted in the CIELAB color space at the Munsell values 3, 5 and 7. They are compared with the computed hue geodesics and chromas contours of above mentioned four formulas.

Method

Riemannian Metric

In a Riemannian space, a positive definite symmetric metric tensor g_{ik} is a function that is used to compute the infinitesimal distance between any two points. So, the length of an infinitesimal curve between two points is expressed by a quadratic differential form as given below:

$$ds^2 = g_{11}dx^2 + 2g_{12}dxdy + g_{22}dy^2. \tag{1}$$

The matrix form of Equation (8) is

$$ds^2 = \begin{bmatrix} dx & dy \end{bmatrix} \begin{bmatrix} g_{11} & g_{12} \\ g_{12} & g_{22} \end{bmatrix} \begin{bmatrix} dx \\ dy \end{bmatrix}, \tag{2}$$

and

$$g_{ik} = \begin{bmatrix} g_{11} & g_{12} \\ g_{21} & g_{22} \end{bmatrix} \tag{3}$$

where ds is the distance between two points, dx and dy are differentials of the coordinates x and y and g_{11}, g_{12} and g_{22} are the coefficients of the metric tensor g_{ik}. Here, the coefficient g_{12} is equal to the coefficient g_{21} due to symmetry.

In a two dimensional color space, the metric g_{ik} gives the intrinsic properties of the color space. Specifically, the metric represents chromaticity differences of any two colors measured along any curve of the surface. Riemannian metrics of the CIELAB, the CIELUV, and the OSA-UCS ΔE_E can be derived in a similar way because they are simply identity metrics in their respective color spaces. The Riemannian approximation of CIEDE2000 on the other hand is a non-Euclidean metric, so its Riemannian metric constitute weighting functions, parametric functions and rotation term. The detailed explanation about this as well as the derivation of Riemannian metrics of above color difference formulas can be found in the authors' previous article [30].

Jacobian Transformation

The quantity ds^2 in Equation (1) is called the first fundamental form and it gives the metric properties of a surface. Now, suppose that x and y are related to another pair of coordinates u and v. The metric tensor g_{ik} can be expressed in terms of the new coordinates as g'_{ik}. In analogy with Equation (3), it is written as:

$$g'_{ik} = \begin{bmatrix} g'_{11} & g'_{12} \\ g'_{21} & g'_{22} \end{bmatrix}. \tag{4}$$

Now, the new metric tensor g'_{ik} is related to g_{ik} via the matrix equation as follows:

$$\begin{bmatrix} g'_{11} & g'_{12} \\ g'_{21} & g'_{22} \end{bmatrix} = \begin{bmatrix} \frac{\partial x}{\partial u} & \frac{\partial x}{\partial v} \\ \frac{\partial y}{\partial u} & \frac{\partial y}{\partial v} \end{bmatrix}^T \begin{bmatrix} g_{11} & g_{12} \\ g_{21} & g_{22} \end{bmatrix} \begin{bmatrix} \frac{\partial x}{\partial u} & \frac{\partial x}{\partial v} \\ \frac{\partial y}{\partial u} & \frac{\partial y}{\partial v} \end{bmatrix}, \tag{5}$$

where the superscript T denotes the matrix transpose, and the matrix

$$J = \frac{\partial(x,y)}{\partial(u,v)} = \begin{bmatrix} \frac{\partial x}{\partial u} & \frac{\partial x}{\partial v} \\ \frac{\partial y}{\partial u} & \frac{\partial y}{\partial v} \end{bmatrix} \tag{6}$$

is the Jacobian matrix for the coordinate transformation, or, simply, the Jacobian. Applying the Jacobian method, one can transform color vectors and metric tensors from one color space to another space easily. For example, the CIELUV metric tensor can be transformed into the CIELAB color space by computing the following Jacobians:

$$g_{\Delta E^*_{uv}} = \frac{\partial(X,Y,Z)}{\partial(L^*,a^*,b^*)}^T \frac{\partial(L^*,u^*,v^*)}{\partial(X,Y,Z)}^T I \frac{\partial(L^*,u^*,v^*)}{\partial(X,Y,Z)} \frac{\partial(X,Y,Z)}{\partial(L^*,a^*,b^*)} \tag{7}$$

where $\partial(X,Y,Z)/\partial(L^*,a^*,b^*)$ and $\partial(L^*,u^*,v^*)/\partial(X,Y,Z)$ are the Jacobian metrics and I is an identity matrix in Equation (7). For a detailed derivation of the Jacobians involved, it is referred to the authors' previous paper [30].

The Geodesic Equation

The line element is often written as:

$$ds^2 = g_{ik}dx^i dx^k. \tag{8}$$

Here, Einstein's summation convention which indicates summation over repeated indices, $a^i b_i = \sum_i a^i b_i$ is used. If we consider two points p_1 and p_2, the distance between the two points along a given path is given by the line integral:

$$s = \int_{p_1}^{p_2} ds = \int_{p_1}^{p_2} (g_{ik} dx^i dx^k)^{\frac{1}{2}}. \tag{9}$$

The shortest distance between p_1 and p_2 can be obtained by minimizing s with respect to the path. This path is called the geodesic. Using variational calculus approach and introducing the Lagrangian $L[dx^i/d\lambda, x^i] = \sqrt{g_{ik} \, dx^i/d\lambda \, dx^k/d\lambda}$, Equation (9) in terms of the variation of distance s with path is

$$\delta s = \int_{p_1}^{p_2} \delta L \, d\lambda. \tag{10}$$

where λ is a variable that parametrizes the path. The distance s will be minimum when $\delta s = 0$. From Equation (10) with the criteria of minima, we can obtain the Euler-Lagrange equation in the following form (the detail mathematical derivations can be found in Cohen's text [31]):

$$\frac{\partial L}{\partial x^i} - \frac{d}{d\lambda} \left(\frac{\partial L}{\partial (dx^i/d\lambda)} \right) = 0 \tag{11}$$

From Equation (11), the geodesic equation is derived and is expressed as below:

$$\frac{d^2 x^i}{ds^2} + \Gamma^i_{jk} \frac{dx^j}{ds} \frac{dx^k}{ds} = 0. \tag{12}$$

where Γ^i_{jk} are called Christoffel symbols and are defined in terms of the metric tensor as follows:

$$\Gamma^i_{jk} = \frac{1}{2} g^{i\nu} \left[\frac{\partial g_{j\nu}}{\partial x^k} + \frac{\partial g_{k\nu}}{\partial x^j} - \frac{\partial g_{jk}}{\partial x^\nu} \right]. \tag{13}$$

Here, $g^{i\nu}$ is the inverse of the metric $g_{i\nu}$ satisfying $g^{i\nu} g_{k\nu} = \delta^i_k$. Here, δ^i_k is the Kronecker delta which vanishes for $i \neq k$. Equation (12) can be written in terms of the first order ordinary differential equations as follows:

$$\begin{aligned} \frac{dx^i}{ds} &= u^i \\ \frac{du^i}{ds} &= -\Gamma^i_{jk} u^j u^k \end{aligned} \tag{14}$$

In two dimensions, for $\Gamma^i_{jk}(i, j, k = 1, 2)$, Equation (14) is expressed as:

$$\begin{aligned} \frac{dx^1}{ds} &= u^1 \\ \frac{dx^2}{ds} &= u^2 \\ \frac{du^1}{ds} &= -\Gamma^1_{11}(u^1)^2 - 2\Gamma^1_{12} u^1 u^2 - \Gamma^1_{22}(u^2)^2 \\ \frac{du^2}{ds} &= -\Gamma^2_{11}(u^1)^2 - 2\Gamma^2_{12} u^1 u^2 - \Gamma^2_{22}(u^2)^2 \end{aligned} \tag{15}$$

where, the superscript in italics are indices.

The Geodesic Grid Construction

Differential equations as given in Equation (15) need to be solved to compute the hue geodesics as well as the chroma contours of the CIELAB, the CIELUV, the Riemannized ΔE_{00} and the ΔE_E color difference formulas in the CIELAB color space. Analytical solutions for these equations are complex due to their nonlinear nature. The authors use the Runge-Kutta numerical method for computing the hue geodesics and chroma contours of above color difference formulas in the CIELAB color space. This method gives a solution to increase the accuracy of the integration. The step size is taken 10^{-4} to balance a trade off between rounding error and truncation error. Centered difference formulas are used to calculate the partial derivatives of the metric tensors in the expression for the Christoffel symbols in Equation (14).

Hue geodesics of these color difference formulas start from the origin of a^*, b^* to different directions in the CIELAB color space with a fixed value of L^* and they are spaced from each other at constant intervals. In a similar way, chroma contours start from the a^*, b^* origin. They are also evenly spaced along the hue geodesic distance. The hue geodesics and chroma contours form the geodesic grids of the above four color difference formulas.

Results and Discussion

Geodesic grids of four color difference formulas, the CIELAB, the CIELUV, the Riemannized ΔE_{00} and the ΔE_E are computed and drawn in the CIELAB color space by using the technique described in the previous section. The Munsell color order system is used to compare these computed hue geodesics and chroma contours. Figures 1(a)–1(c) show the Munsell chromas and hue circles at the Munsell value 3, 5 and 7. Figures 2, 3 and 4 show the hue geodesics and chroma contours of the CIELAB, the CIELUV, the Riemannized ΔE_{00} and the ΔE_E computed at $L = 30/50/70$, which correspond to the Munsell value 3, 5 and 7 respectively.

The CIELAB formula is defined as a Euclidean metric in the CIELAB color space, so its hue geodesics and chroma contours are straight lines and circles. They are compared with the Munsell chromas and hue circles at different Munsell values as shown in Figures 2(a), 3(a) and 4(a). The computed hue geodesics intersect the Munsell chromas around yellow, green and blue areas. In the red region of the CIELAB space, the hue geodesics follow the same directions as the Munsell chromas. However, the Munsell chromas are curved at high chroma whereas the hue geodesics of the CIELAB formula are straight in the same region. The chroma contours also vary from the Munsell hue circles at the Munsell value 5 and 7, but at the value 3, the chroma contours are closer to the Munsell hue circles at the a^*, b^* origin and the central region of the CIELAB color space.

The CIELUV hue geodesics and chroma contours tend to agree more with the Munsell chromas and hue circles than the ones predicted by the CIELAB formula. But, the geodesic grids of the CIELUV formula do not cover the Munsell chromas and hue circles due to integration instability. It can be seen in Figures 2(b), 3(b) and 4(b). In this case, hue geodesics predicted by the CIELUV formula intersect the Munsell chromas mostly in the third quadrant of the CIELAB space. This result indicates that the CIELUV hue geodesics and

the Munsell chroma differ in the blue-green region of the CIELAB color space. The CIELUV hue geodesics also follow the curvature pattern of the Munsell chromas, and their directions in the red and yellow regions of the CIELAB space are very close to the Munsell chromas. Chroma contours of the CIELUV formula appear elliptical. They are also similar to the Munsell hue circles at the a^*, b^* origin and the central region. However, they do not comply fully in accordance with the Munsell hue circles in the rest of the CIELAB color space.

The Riemannized ΔE_{00} hue geodesics and chroma contours begin from near the a^*, b^* origin. This is due to the nonexistence of the Riemannian metric at $a^* = b^* = 0$. The detailed discussion about difficulty for getting Riemannian metric of the CIEDE2000 can be found in the article of Pant and Farup [30]. Geodesic grids of the Riemannized ΔE_{00} and their comparison with the Munsell hue and chromas at the different Munsell values are shown in Figures 2(c), 3(c) and 4(c). The hue geodesics are more consistent with the Munsell chromas than the hue geodesics predicted by the CIELAB and the CIELUV metrics. However, they do not follow the curvature pattern of the Munsell chroma in the red and yellow regions of the CIELAB color space. In the blue and violet regions, hue geodesics are sharply curved. They are also changing direction of curvature on their path for intermediate chromas in the CIELAB color space (around $C^* \approx 20$). The chroma contours are elliptical in the central region of the CIELAB color space. Their shapes also diverge from circular to notch on their path in the blue and violet regions. In general, they do not match the Munsell hue circles. The authors found that changing direction of hue geodesics along their path as well as the elliptical shape of chroma contours in the central region are due to the G parameter in the CIEDE2000 formula [20]. Figure 5 shows the hue geodesic and chroma contours of the Riemannized ΔE_{00} setting the value of $G = 0$. This improves the problems of the changing direction of the hue geodesics and the elliptical shape of the chroma contours except in the blue region of the CIELAB space. However, the rotation term of the CIEDE2000 formula is accountable for the sharply curved hue geodesics as well as the shifting of chroma contours in the blue region. This finding suggests that correcting chroma in the blue region of the color space can have a diverse effect on the whole color space.

The OSA-UCS based ΔE_E geodesic grid looks somewhat similar to the CIELUV geodesic grid. Figures 2(d), 3(d) and 4(d) show the ΔE_E hue geodesics and chroma contours. They are following more closely to the direction of the Munsell chromas and hue circles. In the blue region, the hue geodesics intersect the planes of the Munsell chroma. Likewise, the shape of ΔE_E chroma contours are similar to the ones predicted by the CIELUV formula, but they appear to be more correct. Chroma contours are similar to the Munsell hue circles in the achromatic region of the CIELAB color space. In this case also, the ΔE_E predicted chroma contours are not matching the Munsell hue circles in the other parts of the CIELAB color space.

Conclusion

Hue geodesics and chroma contours of color difference metrics can be computed in any desired color space with the known Riemannian metric tensors. This technique is successfully shown by computing geodesic grids of the CIELAB,
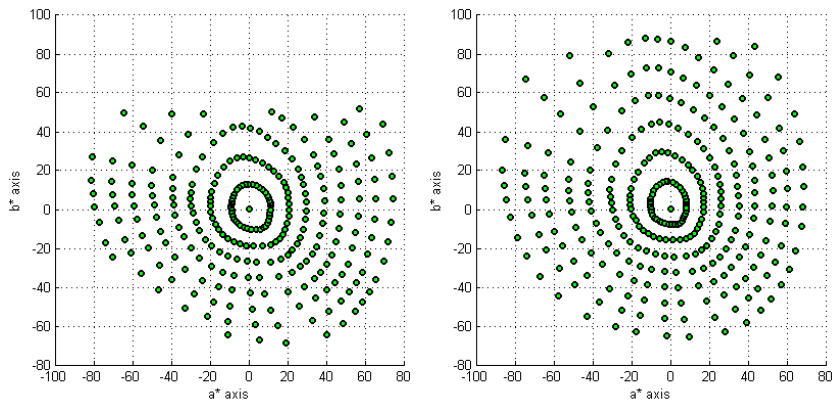
(a) Munsell chromas and hues at value 3. (b) Munsell chromas and hues at value 5.
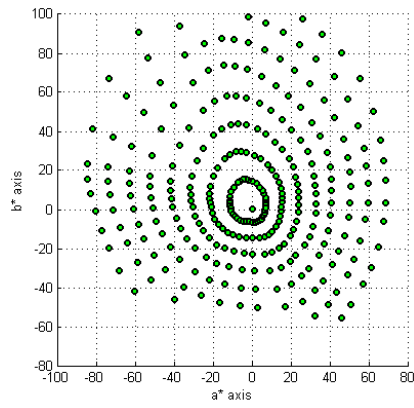
(c) Munsell chromas and hues at value 7.

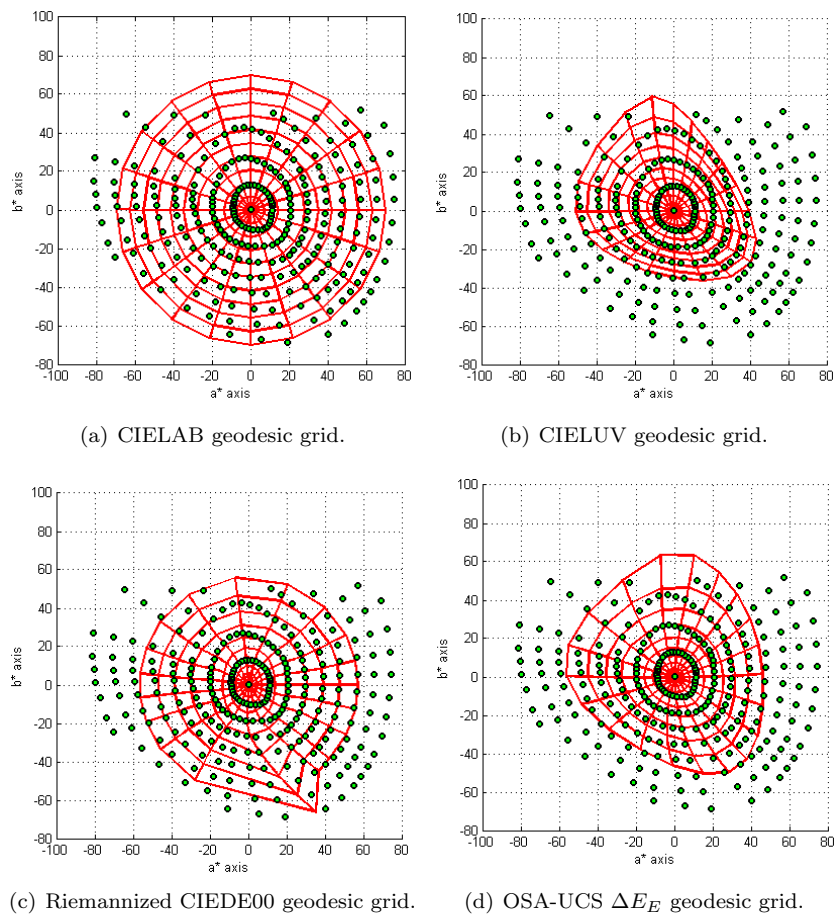Figure 1: Munsell chromas and hues at different Munsell values.

(a) CIELAB geodesic grid.

(b) CIELUV geodesic grid.

(c) Riemannized CIEDE00 geodesic grid.

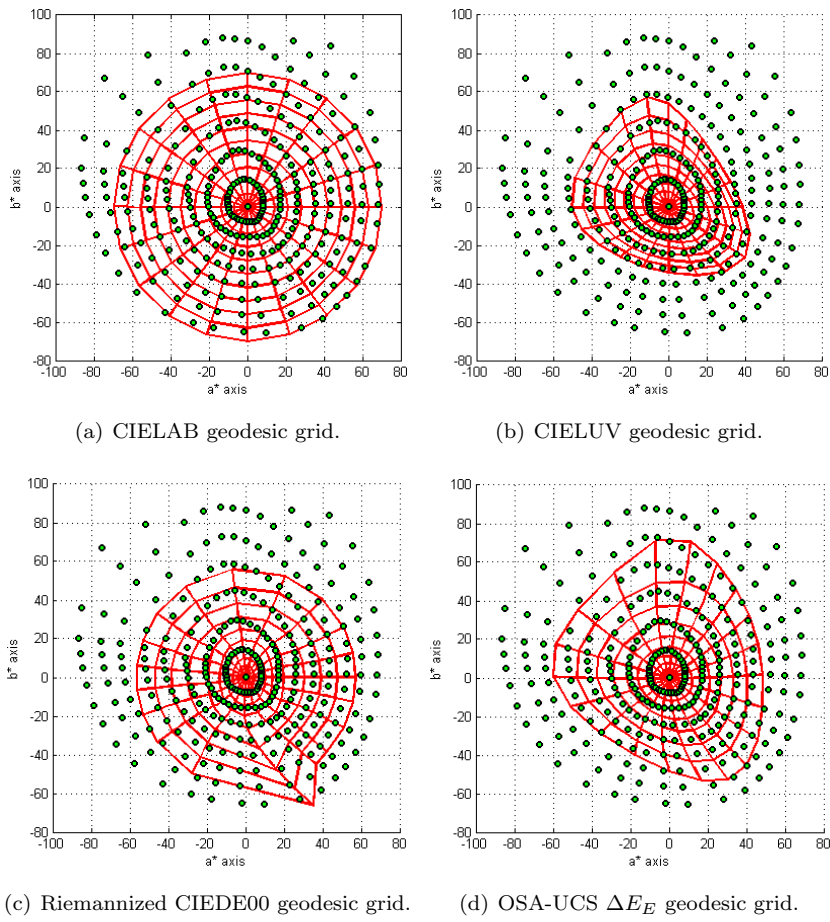(d) OSA-UCS ΔE_E geodesic grid.

Figure 2: Computed geodesic grids of CIELAB, CIELUV, Riemannized CIEDE00 and OSA-UCS ΔE_E in the CIELAB space and compared with the Munsell chromas and hues at the Munsell value 3.

(a) CIELAB geodesic grid.

(b) CIELUV geodesic grid.

(c) Riemannized CIEDE00 geodesic grid.

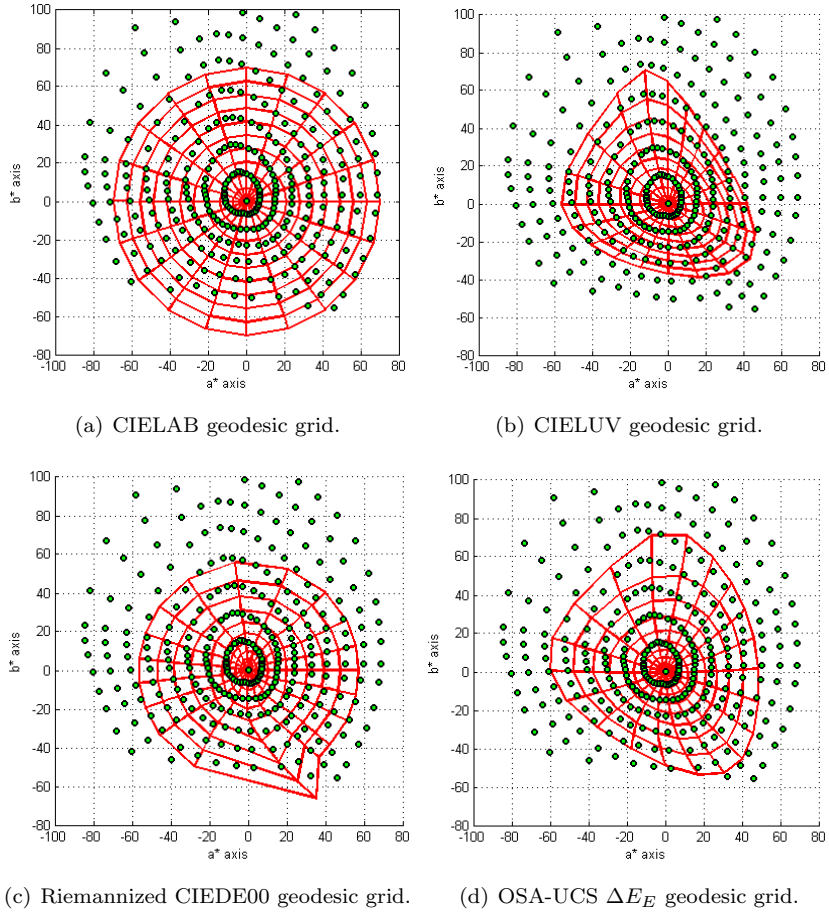(d) OSA-UCS ΔE_E geodesic grid.

Figure 3: Computed geodesic grids of CIELAB, CIELUV, Riemannized CIEDE00 and OSA-UCS ΔE_E in the CIELAB space and compared with the Munsell chromas and hues at the Munsell value 5.

(a) CIELAB geodesic grid.

(b) CIELUV geodesic grid.

(c) Riemannized CIEDE00 geodesic grid.

(d) OSA-UCS ΔE_E geodesic grid.

Figure 4: Computed geodesic grids of CIELAB, CIELUV, Riemannized CIEDE00 and OSA-UCS ΔE_E in the CIELAB space and compared with the Munsell chromas and hues at the Munsell value 7.
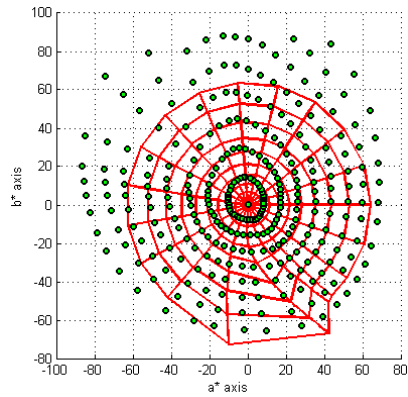

Figure 5: Riemannized CIEDE00 geodesic grid with $G = 0$.

11

CIELUV, Riemannized CIEDE00 and OSA-UCS ΔE_E color difference formulas with the fixed value of lightness L^* in the CIELAB color space. Comparisons of the geodesic grids of these formulas with the Munsell hues and chromas at the Munsell values 3, 5 and 7 show that none of these four formulas can precisely fit the Munsell data. It is interesting to note that the latest color difference formulas like the OSA-UCS ΔE_E and the Riemannized CIEDE2000 do not show better performance to predict hue geodesics and chroma contours than the conventional CIELAB and CIELUV color difference formulas. These findings also suggest that the distribution of hue geodesics and chroma contours of the above four color difference formulas are weak to predict perceptual color attributes in all over the color space even though their quantitative color difference measures are good.

Acknowledgments

References

[1] D. MacAdam, "Visual sensitivities to color differences in daylight," J. Optical Society of America **32**, 247–274 (1942).

[2] W. Brown, "Colour discrimination of twelve observers," J. Optical Society of America **47**, 137–143 (1957).

[3] M. R. Luo and B. Rigg, "Chromaticity-discrimination ellipses for surface colours," Color Res. Appl. **11**, 25–42 (1986).

[4] R. Berns, D. H. Alman, L. Reniff, G. Snyder, and M. Balonon-Rosen, "Visual determination of suprathreshold color-difference tolerances using probit analysis," Color Res. Appl. **16**, 297–316 (1991).

[5] K. Chickering, "Optimization of the MacAdam modified 1965 friele color-difference formula," J. Optical Society of America **57**, 537 (1967).

[6] H. von Helmholtz, "Das psychophysische Gesetz auf die Farbunterschiede trichromatischer Auge anzuwenden," Psychol. Physiol. Sinnesorgane **3**, 1–20 (1892).

[7] E. Schrödinger, "Grundlinien einer Theorie der Farbenmetrik im Tagessehen," Annalen der Physik **4**, 397–426 (1920).

[8] E. J. Muth and C. G. Persels, "Constant-brightness surfaces generated by several color-difference formulas," Optical Society of America **61**, 1152–1154 (1971).

[9] A. K. Jain, "Color distance and geodesics in color 3 space," J. Optical Society of America **62**, 1287–1291 (1972).

[10] C. L. Sanders and G. Wyszecki, "Corrleate for lightness in terms of cie-tristimulus values. part i," J. Optical Society of America **47**, 398–404 (1957).

[11] J. Vos and P. Walraven, "An analytical description of the line element in the zone fluctuation model of color vision," J. Vision Research **12**, 1345–1365 (1972).

[12] J. Vos, "From lower to higher colour metrics: a historical account," Clinical and Experimental Optometry **89**, 348–360 (2006).

[13] J. Vos and P. Walraven, "Back to Helmholtz," Color Res. Appl. **16**, 355–359 (1991).

[14] G. Wyszecki and W. Stiles, *Color Science: Concepts and Methods, Quantitative Data and Formula* (John Wiley and Sons, New York, 2000), 2nd ed.

[15] T. Kohei, J. Chao, and R. Lenz, "On curvature of color spaces and its implications," in "5th European Conference on Colour in Graphics, Imaging, and Vision, CGIV 2010," (2010).

[16] J. Chao, I. Osugi, and M. Suzuki, "On definitions and construction of uniform color space," in "2nd European Conference on Colour in Graphics, Imaging and Vision (CGIV 2004)," (2004), pp. 55–60.

[17] J. Chao, R. Lenz, D. Matsumoto, and T. Nakamura, "Riemann geometry for color characterization and mapping," in "In: Proc. CGIV , IS&T, Springfield," (2008).

[18] S. Ohshima, R. Mochizuki, J. Chao, and R. Lenz, "Colour reproduction using riemann normal coordinates," in ""Computational Color Imaging " 2nd International workshop , CCIW," (Springer-Verlag, 2009), pp. 140–149.

[19] CIE, "Recommendations on uniform colour spaces, colour difference equations and psychometric color terms," Tech. Rep. 15, CIE Central Bureau, Vienna (1978).

[20] M. Luo, G. Cui, and B. Rigg, "The development of the CIE2000 colour difference formula," Color Res. Appl. **26**, 340–350 (2001).

[21] C. Oleari, M. Melgosa, and R. Huertas, "Euclidean colour difference formula for small-medium colour differences in log-compressed OSA-UCS space," J. Optical Society of America **26**, 121–134 (2009).

[22] CIE, "Industrial colour difference evaluation," Tech. Rep. 116, CIE Central Bureau, Vienna (1995).

[23] D. Kim and J. Nobbs, "New weighting functions for the weighted CIELAB colour difference formula," in "Proceedings of AIC Colour," (AIC, Kyoto, 1997), pp. 446–449.

[24] CIE, "Improvement to industrial color–difference evaluation," Tech. Rep. 142, CIE central bureau, Vienna (2001).

13

[25] J. Gay and R. Hirschler, "Field trials for CIEDE2000: Correlation of visual and instrumental pass/fail decisions in industry." Tech. Rep. ISBN 390190621, 25th, The CIE Session, San Diego (2003).

[26] M. Melgosa, R. Huertas, and R. S. Berns, "Performance of recent advanced color difference fromulae using the standardized residual sum of squares index," J. Optical Society of America **25**, pp. 1828–1834 (2008).

[27] P. Urban, M. R. Rosen, and R. S. Berns, "Embedding non-euclidean color spaces into euclidean color spaces with minimal isometric disagreement," Optical Society of America **27** (2007).

[28] R. G. Kuehni, *Color Space and its Division* (John Wiley and Sons, New York, 2003).

[29] V. H. G., "Die Berechnung grosser farbabst ́ande in nichteuklidischen Farbr ́aumen." Die Farbe **44**, 1–45 (1998).

[30] D.R.Pant and I. Farup, "Riemannian formulation and comparison of color difference formulas," Color Res. Appl.(accepted) (2011).

[31] H. Cohen, *Mathematics for Scientists and Engineers* (Prentice-Hall International Editions, 1992).